 Human Molecular Genetics, 1999, Vol. 8, No. 3 387–396

ARTICLE

Truncated CBP protein leads to classical Rubinstein–Taybi syndrome phenotypes in mice: implications for a dominant-negative mechanism

Yuichi Oike[1,2], Akira Hata[3], Takayoshi Mamiya[4], Tadashi Kaname[1], Yukihiro Noda[4], Misao Suzuki[5], Hirofumi Yasue[2], Toshitaka Nabeshima[4], Kimi Araki[1] and Ken-ichi Yamamura[1,*]

[1]Department of Developmental Genetics, Institute of Molecular Embryology and Genetics, [2]Department of Cardiovascular Medicine and [5]Laboratory of Transgenic Technology, Kumamoto University School of Medicine, Kuhonji 4-24-1, Kumamoto 862-0976, Japan, [3]Department of Public Health, Hokkaido University School of Medicine, Sapporo 060-8638, Japan and [4]Department of Neuropsychopharmacology and Hospital Pharmacy, Nagoya University School of Medicine, Nagoya 466-8560, Japan

Received September 2, 1998; Revised and Accepted November 30, 1998

A mouse model of Rubinstein–Taybi syndrome (RTS) was generated by an insertional mutation into the cyclic AMP response element-binding protein (CREB)-binding protein (CBP) gene. Heterozygous CBP-deficient mice, which had truncated CBP protein (residues 1–1084) containing the CREB-binding domain (residues 462–661), showed clinical features of RTS, such as growth retardation (100%), retarded osseous maturation (100%), hypoplastic maxilla with narrow palate (100%), cardiac anomalies (15%) and skeletal abnormalities (7%). Truncated CBP is considered to have been acting during development as a dominant-negative inhibitor to lead to the phenotypes of RTS in mice. Our studies with step-through-type passive avoidance tests and with fear conditioning test showed that mice were deficient in long-term memory (LTM). In contrast, short-term memory (STM) appeared to be normal. These results implicate a crucial role for CBP in mammalian LTM. Our *CBP*$^{+/-}$ mice would be an excellent model for the study of the role of CBP in development and memory storage mechanisms.

INTRODUCTION

Rubinstein–Taybi syndrome (RTS) is an autosomal dominant well-delineated dysmorphic syndrome characterized by retarded growth and mental function (94 and 100%), broad thumbs and toes (100%), retarded osseous maturation (94%), microcephaly (84%) and typical craniofacial abnormalities including hypoplastic maxilla with narrow palate (100%), downward slanting palpebral fissures (100%) and large anterior fontanel (64%). Other clinical problems include electroencephalogram abnormalities (60%), cardiac anomalies (33%) and occasional skeletal and eye abnormalities (1). The prevalence of this syndrome has been estimated to be 1 in 125 000 living newborns (2) and also has been estimated to account for as many as 1 in 300 cases of institutionalized mentally retarded subjects (3).

Recently, mutations in the gene encoding the cyclic AMP response element-binding protein (CREB)-binding protein (CBP) (4) were found to cause RTS (5). CBP is a 2441 amino acid 265 kDa nuclear protein that is a coactivator molecule for a number of transcription factors including CREB, c-Fos, c-Jun, c-Myb and several nuclear receptors (6–11). However, the nature of the anatomical and physiological defects in RTS patients in relation to *CBP* mutations is still poorly understood. To answer these questions, a *CBP*$^{+/-}$ mouse model would be valuable. Tanaka *et al.* (12) generated a *CBP*$^{+/-}$null mutant mouse in which amino acids 29–265 of CBP were replaced with a targeting vector using homologous recombination. However, those null mutant mice exhibited only growth retardation (7/21 mice) and skeletal abnormalities, such as large anterior fontanel (14/21) and distinct holes in the xiphoid process (6/21).

Two different mechanisms by which CBP defects lead to RTS phenotypes can be considered: haplo-insufficiency and dominant-negative. For a haplo-insufficiency mechanism, two functional copies of the gene are required to produce sufficient product for normal development. For a dominant-negative mechanism, abnormal product derived from the mutant allele inhibits the wild-type product. Petrij *et al.* (5) claimed that

*To whom correspondence should be addressed. Tel: +81 96 373 5319; Fax: +81 96 373 5321; Email: yamamura@gpo.kumamoto-u.ac.jp

haplo-insufficiency seems to be the more likely explanation because both truncated mutants and null mutants cause human RTS. However, microinjection experiments of the CBP CREB-binding domain (residues 455–679) into mammalian fibroblast nuclei blocked transcriptional activation of a CRE–*lacZ* reporter gene in a dominant-negative fashion (11,13). Taken together with the fact that null mutant mice (12) exhibit only mild RTS phenotypes, it is possible that both mechanisms play a role in the development of RTS phenotypes at least in mice.

In the present study, we generated *CBP*$^{+/-}$ mice with truncated CBP protein (residues 1–1084; residues 1085–2441 are not present) containing the CREB-binding domain (residues 462–661). Our *CBP*$^{+/-}$ mice showed growth retardation (100/100 mice, 100%), poor locomotor activity (100%), long-term memory (LTM) deficits (100%), retarded osseous maturation (100%), large anterior fontanel (100%), hypoplastic maxilla with narrow palate (100%), cardiac anomalies (17%), skeletal abnormalities (7%) and occasional seizures (data not yet analyzed). However, broad thumbs and toes were not observed. Since both Tanaka *et al.* (12) and ourselves used the TT2 embryonic stem (ES) cell line (14) for mutant generation, and C57BL/6 for backcross mating, a dominant-negative effect is the most plausible explanation for the differences. Furthermore, the defect in LTM acquisition was observed in our *CBP*$^{+/-}$ mice, implicating a significant role for CBP in mammalian LTM.

RESULTS

Generation of CBP-deficient mice

In order to identify unique genes associated with development in mice, we have performed gene trapping (15,16) using the pU-San vector with the β-geo reporter gene (Fig. 1a). We have generated several insertional mutant mouse lines through production of chimeric mice. Of these lines, the no. 112 line with heterozygotes showing apparent growth retardation was chosen for further analyses. Southern blot analysis with a vector fragment as a probe indicated only a single copy of the vector integrated (data not shown). Analyses of the mutated genomic region revealed that the insertion occurred in an intron of the *CBP* gene located between the exons containing nucleotides 3064–3253 and 3254–3373 (Fig. 1b). Restriction mapping and Southern blot analyses showed that no gross deletion occurred at the inserted region. The chimeras were mated with C57BL/6 females to generate F_1 *CBP*$^{+/-}$ mice. *CBP*$^{+/-}$ mice were identified by Southern blot analysis (Fig. 1c). The homozygous mutants died *in utero* between 9.5 and 10.5 days post-coitum (d.p.c.) (Y. Oike *et al.*, submitted for publication).

Western blot analysis of brain homogenate of *CBP*$^{+/-}$ mice with N-terminal-specific antibodies detected a smaller fragment in addition to the wild-type product (Fig. 1d). However, with C-terminal-specific antibodies, the smaller fragment was not detected (data not shown). This 121 kDa fragment which contains the CREB-binding domain is the exact expected size of the CBP truncated protein (CBP amino acids 1–1084 + 71 amino acids from the vector) (Fig. 1e).

Phenotypes of *CBP*$^{+/-}$ mice

CBP$^{+/-}$ mice showed severe intrauterine growth retardation in both weight and height, although the postnatal weight gain for the mice is comparable with *CBP*$^{+/+}$ mice (Fig. 2a). As shown in Figure 2b, *CBP*$^{+/-}$ mice exhibit a broad nasal bridge, short nose and hypoplastic maxilla. Radiological examination of the skeletal systems of F_2 +/+ and +/– littermates (n = 30 each) was performed. Retarded osseous maturation, large anterior fontanel (studied in 19.5 d.p.c. fetuses; data not shown), short premaxilla and maxillary bone, and hypoplastic nasal bone were observed in all *CBP*$^{+/-}$ mice, but not in *CBP*$^{+/+}$ mice (Fig. 2c and d). In addition, oligodactyly (1/30) and severe scoliosis (1/30) were noted only in *CBP*$^{+/-}$ mice (data not shown). Bone and cartilage stained specimens were also analyzed and they confirmed the above data (data not shown). The observation that some of the F_2 *CBP*$^{+/-}$ pups died within several days prompted us to analyze cardiac formation of 19.5 d.p.c. fetuses. As shown in Table 1, nine out of 54 *CBP*$^{+/-}$ fetuses (16.6%) had cardiac anomalies [seven ventricular septal defect (VSD), one atrial septal defect and one bicuspid valve; no overlapping anomalies], while none of the *CBP*$^{+/+}$ mice had any cardiac abnormalities. All the VSDs observed in *CBP*$^{+/-}$ fetuses belong to the membranous type (Fig. 3). In addition, seizures were observed in at least two *CBP*$^{+/-}$ mice.

Table 1. Types, numbers and incidence (%) of heart anomalies in *CBP*$^{+/+}$ and *CBP*$^{+/-}$ littermates

	CBP$^{+/+}$ (n = 56) No. (%)	*CBP*$^{+/-}$ (n = 54) No. (%)
Fetuses	56	54
Heart anomalies	0 (0)	9 (16.6)[a]
Ventricular septal defect	0 (0)	7 (12.9)[a]
Atrial septal defect	0 (0)	1 (1.8)
Bicuspid valve	0 (0)	1 (1.8)

Fourteen litters were analyzed.
[a]$P < 0.01$ versus *CBP*$^{+/+}$ mice.

Locomotor activity, memory acquisition, short- and long-term memory

Locomotor activity was measured by photocell counter (17) and revealed that *CBP*$^{+/-}$ mice are significantly less active than *CBP*$^{+/+}$ mice in a dark environment but not in a light environment (data not shown). Hypolocomotion in *CBP*$^{+/-}$ mice in the dark environment was observed throughout the entire 60 min in the vertical activity, but only in the first 5 min in the horizontal activity (Fig. 4a).

To evaluate memory acquisition, short-term memory (STM), LTM and spatial learning, we employed four behavioral studies: step-through-type passive avoidance (18,19), Y-maze (18, 20–22), fear conditioning (23) and water maze tests (19).

In the step-through-type passive avoidance test, assessing memory acquisition and LTM, a mouse was placed in a cage consisting of light and dark compartments, and received an electric shock when it entered the dark chamber to make it stay in the light chamber for a constant time during the training trials. After several days, the step-through latencies to the dark chamber were recorded in the retention trials. In the acquisition trials, there were no differences between the mutant and wild-type mice either in the step-through latency on first training or in the number of trials required to learn the task (Fig. 4c). The number of training trials in the acquisition trials and the step-through latency in the

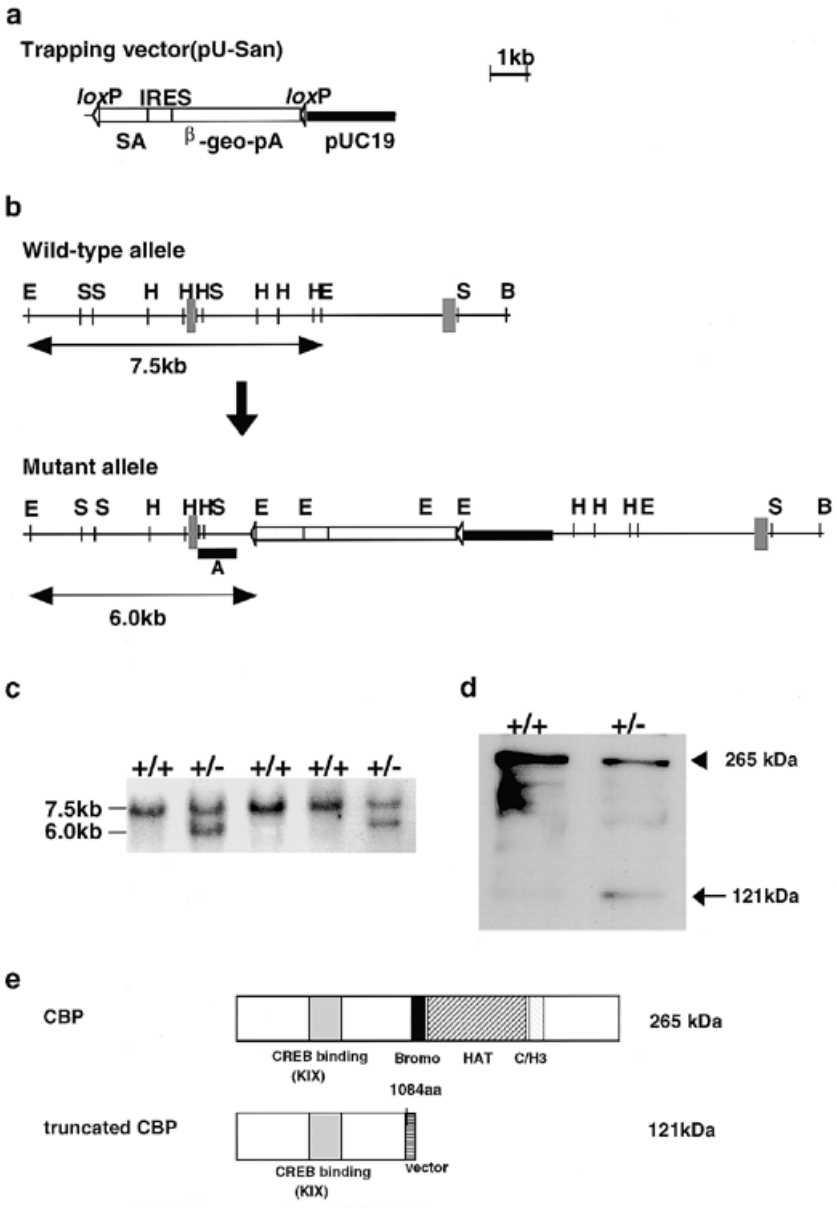

Figure 1. Generation of heterozygous CBP mutant mice (*CBP*$^{+/-}$). (**a**) Structure of the trapping vector. The two *lox*P sequences, splice acceptor region (SA), internal ribosomal entry site (IRES), β-galactosidase/neomycin phosphotransferase fused gene and an SV40 polyadenylation sequence (β-geo-PA), and pUC19 vector sequence are indicated. (**b**) The wild-type *CBP* and mutant alleles. The gray boxes represent exons. Restriction enzyme sites (B, *Bam*HI; E, *Eco*RI; H, *Hin*dIII; S, *Sph*I) are indicated. The Southern blot probe used, solid box A, and the size of the *Eco*RI fragments, containing the indicated exon of nucleotide 3064–3253, hybridizing with this probe, are indicated. (**c**) Southern blot analysis of mouse genomic DNA. Mouse tail DNA was digested with *Eco*RI and hybridized with probe A. The wild-type 7.5 kb band and the mutant 6.0 kb band, and wild-type homozygous +/+ and heterozygous mutant +/– lanes are indicated. (**d**) Immunodetection of CBP protein. Extracts (30 μg protein) from the brains of adult mice were used for western blotting with N-terminal-specific anti-CBP antibodies (A-22). An arrowhead indicates the 265 kDa wild-type CBP protein. An arrow indicates the truncated form of CBP at 121 kDa. (**e**) Schematic diagram of wild-type and truncated CBP. Functional domains as well as vector-derived fusion product are indicated.

retention trials were used as the index of acquisition and retention of training experience, respectively. Twenty four hours later, the step-through latency of CBP mutant mice was significantly shorter than that of wild-type mice (Fig. 4d). At 3 and 5 days after training, the latency of wild-type mice shortened significantly compared with that of the first day. There is no difference between the latencies of mutant mice 1, 3 and 5 days after training. These results suggest that CBP plays an important role in LTM, but not in acquisition. In the step-through-type passive avoidance test, to remove the possibility of the threshold difference for electronic shock between the *CBP*$^{+/+}$ and *CBP*$^{+/-}$ groups, the thresholds for flinch (0.024 ± 0.001 versus 0.022 ± 0.002 mA) and jumping (0.155 ± 0.017 versus 0.133 ± 0.039 mA) were measured, but no significant differences were found.

Working memory, classified as STM, is thought to underlie the alternation behavior in the Y-maze test. Neither the alternation

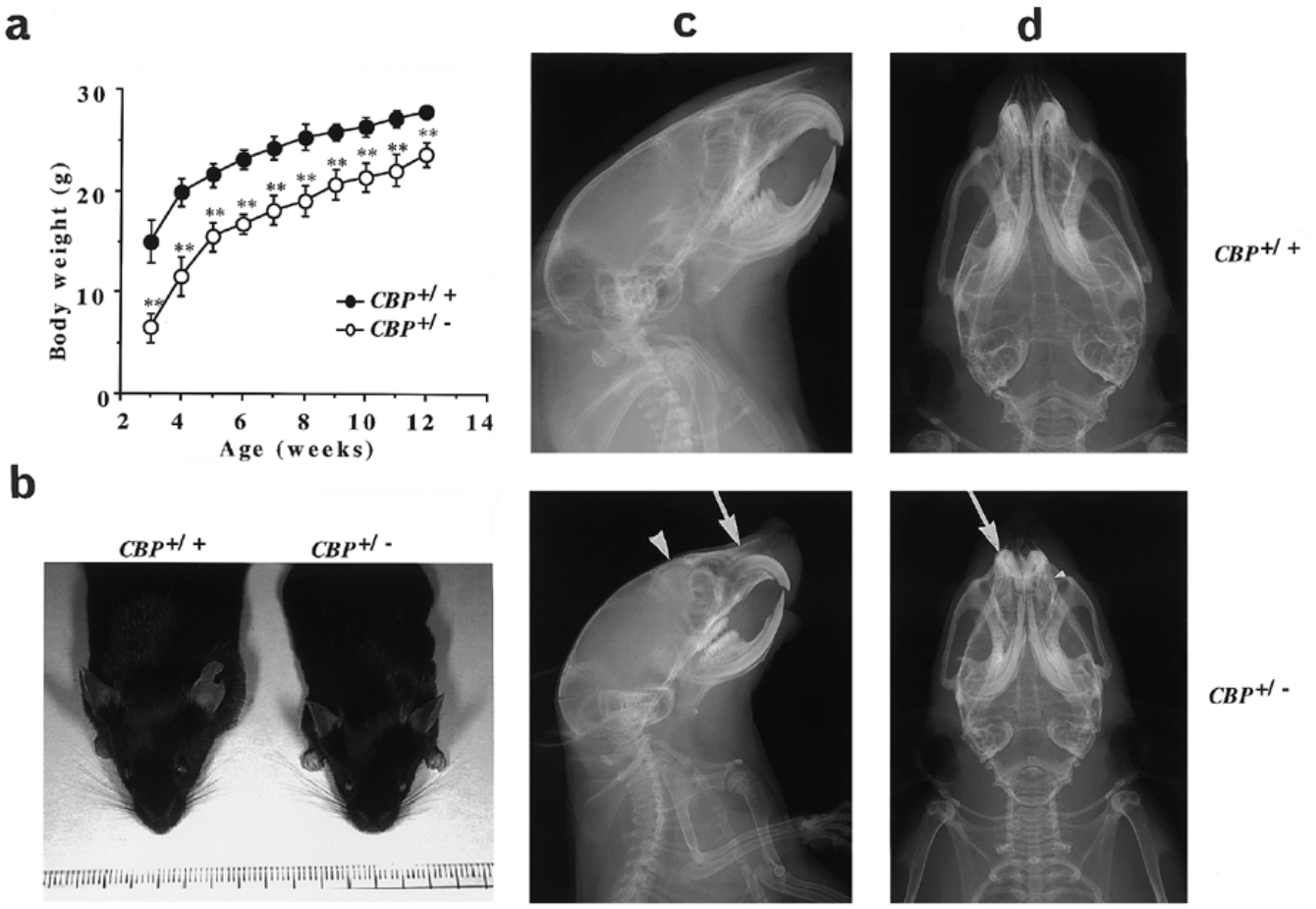

Figure 2. Phenotypes of *CBP*$^{+/-}$mice (compared with wild-type littermates). Only male data are shown as no significant male/female differences were observed. Data shown are means ± SEM. (**a**) Growth curves of *CBP*$^{+/+}$ mice and *CBP*$^{+/-}$littermates (n = 15 each). (*P < 0.05, **P < 0.01 versus *CBP*$^{+/+}$ mice). (**b**) Facial appearance of *CBP*$^{+/+}$ and *CBP*$^{+/-}$ mice. Note the broad nasal bridge, short nose and hypoplastic maxilla of the *CBP*$^{+/-}$ mouse. (c and d) Radiographs of 8-week-old *CBP*$^{+/+}$ mice and *CBP*$^{+/-}$littermates; (**c**) lateral view, (**d**) anterio-posterior view. The large arrowhead indicates widening of the frontal bone. Arrows and a small arrowhead indicate the hypoplastic nasal and premaxilla bones.

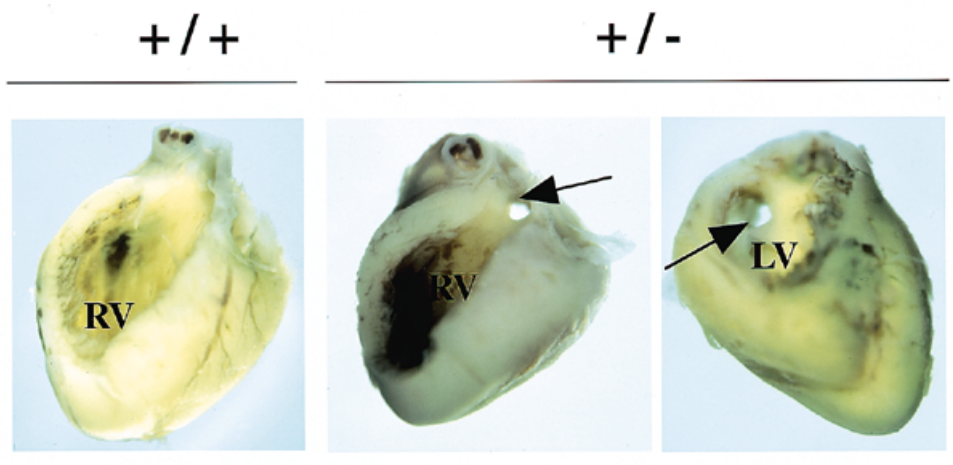

Figure 3. Appearance of a *CBP*$^{+/+}$ normal heart (left) and *CBP*$^{+/-}$heterozygous hearts (middle and right). Note the ventricular septal defect of *CBP*$^{+/-}$heterozygous hearts. The defect (arrow) is located in the membranous region of the ventricular septal wall. LV, left ventricle; RV, right ventricle.

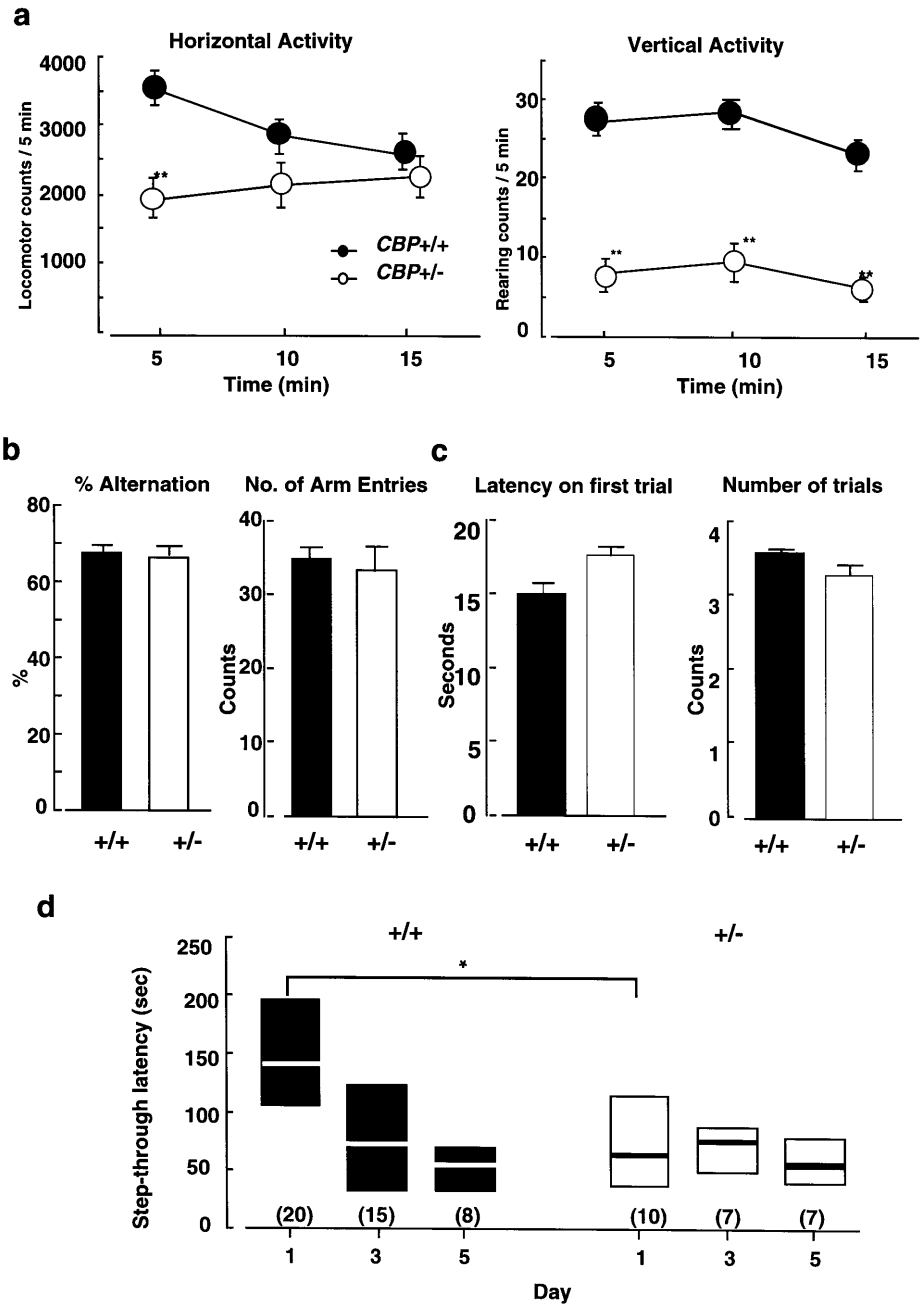

Figure 4. Behavioral and learning analyses of *CBP*$^{+/+}$ mice and *CBP*$^{+/-}$ littermates. Data shown are means ± SEM. (**a**) Locomotor activity, both horizontal and vertical, was determined as the locomotion counts per mouse and expressed as the cumulative counts over 5 min. The data of the first 15 min of the 60 min observation period are shown. Numbers in parentheses show the numbers of animals tested. Note the horizontal hypolocomotion in *CBP*$^{+/-}$ mice during the first 5 min. Note the vertical hypolocomotion in *CBP*$^{+/-}$ mice during the observation periods. (**b**) Normal response of spontaneous alternation behavior studied by Y-maze. There was no significant difference between *CBP*$^{+/+}$ mice and *CBP*$^{+/-}$ littermates in the alternation percentages and the number of arm entries. The numbers of *CBP*$^{+/+}$ mice and *CBP*$^{+/-}$ littermates tested were 19 and 14, respectively. (c and d) Performance in the multiple-trial passive avoidance test of *CBP*$^{+/+}$ mice and *CBP*$^{+/-}$ littermates. (**c**) Step-through latency of mutant (+/–) and wild-type (+/+) mice on the acquisition trials. Number of trials in the acquisition trials. There were no significant differences between the two groups of mice in the step-through latency on the first trial and the number of trials required to reach the criterion of staying in the light compartment for 120 s. (**d**) Step-through latencies in the retention trials performed 1, 3 and 5 days after the acquisition trials. The step-through latencies of the mutant mice were significantly shortened compared with those of wild-type mice. Data were expressed as the median and interquartile ranges, which are distances between the first quartile (25th percentile) and third quartile (75th percentile). The latency of *CBP*$^{+/-}$ mice was significantly shorter than that of *CBP*$^{+/+}$ littermates. **P* < 0.05, ***P* < 0.01 versus *CBP*$^{+/+}$ mice.

behavior nor the total arm entries of *CBP*$^{+/-}$ mice were different from those of *CBP*$^{+/+}$ mice (Fig. 4b), showing that the CBP mutation does not affect STM.

A fear conditioning test in two parts, one for contextual and one for cued conditioning, was also performed to evaluate STM and LTM. As described by Bourtchuladze *et al.* (23), this test

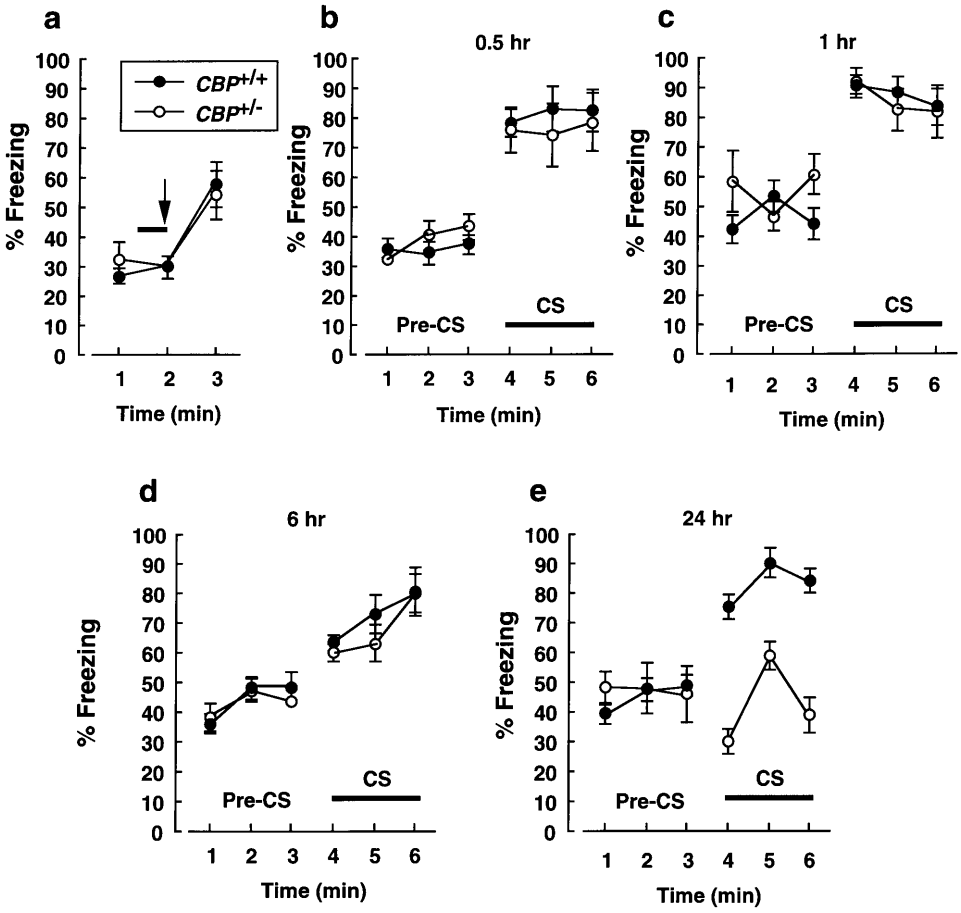

Figure 5. Cued conditioning. (**a**) *CBP*$^{+/+}$ mice and *CBP*$^{+/-}$ littermates from groups 1, 2, 3 and 4 were given a single training trial. A solid line indicates the duration of the tone (CS), while the arrow indicates the 2 s shock (US). Since experiments with all four groups were done in a balanced manner and since the training procedure was identical for all groups, (a) represents pooled training data (n = 32 *CBP*$^{+/+}$ wild type mice and n = 20 *CBP*$^{+/-}$ mutant mice) from all four groups. (**b**–**e**) Groups 1–4 (*CBP*$^{+/+}$ wild type mice, n = 8, and *CBP*$^{+/-}$ mutant mice, n = 5, respectively) were tested at the indicated time points following the cued conditioning trial (a). ANOVA shows that *CBP*$^{+/-}$ mutant mice (n = 5) expressed significantly less freezing responses than did *CBP*$^{+/+}$ wild-type mice (n = 8) only in the response at 24 h in (e) [$F(1,11) = 12.096$, $P < 0.01$].

examines whether mice associate an unconditioned stimulus (foot shock) with the context (the conditioning chamber itself) or the cue (a tone). As shown in Figure 5, the cued conditioning test showed that the difference between *CBP*$^{+/-}$ and *CBP*$^{+/+}$ mice was observed only at 24 h but not at 0.5, 1.0 or 6 h. In the contextual conditioning test, no differences were observed (data not shown).

A water maze test as reported by Bourtchuladze *et al.* (23) was also performed to test spatial learning. No significant differences were observed (data not shown).

To determine whether the poor performance was attributable to defects in brain structure, *CBP*$^{+/+}$ and *CBP*$^{+/-}$ mice brains were analyzed microscopically; no discernible morphological differences were observed (data not shown). Therefore, neither sensorimotor nor gross neuroanatomical defects can account for the LTM deficit of *CBP*$^{+/-}$ mice.

DISCUSSION

The *CBP*$^{+/-}$ mice generated in this study strongly mimicked the clinical features of RTS. All the abnormal phenotypes in our *CBP*$^{+/-}$ mice, such as growth retardation, retarded osseous maturation, large anterior fontanel, hypoplastic maxilla with narrow palate, other skeletal abnormalities, cardiac anomalies and seizures, are also observed in RTS. Mental retardation, one of the key symptoms in patients with RTS, is still difficult to assess in a mouse model. What we can do to evaluate mental retardation are tests for spontaneous activity and memory storage (17–23), which can be disturbed in mental retardation. Locomotor activity was studied by photocell counter and revealed that *CBP*$^{+/-}$ mice are significantly less active than *CBP*$^{+/+}$ mice. In order to evaluate memory acquisition and retention of *CBP*$^{+/-}$ mice, we employed a Y-maze test (18,20–22), a step-through-type passive avoidance test (18,19) and a fear conditioning test (23). The results showed that *CBP*$^{+/-}$ mice had normal STM, but deficient LTM. CBP may play an important role in the retention and retrieval of learning and memory, rather than in acquisition.

To discuss the mechanisms by which truncated CBP affects LTM, the function of CBP domains has to be considered. CBP is a coactivator for a huge variety of transcription factors, of which only CREB is described as having a role in LTM. Homozygous CREB-deficient mice are reported to have normal STM but deficient LTM (23). Studies in *Aplysia* (24) and *Drosophila*

(25–27) also indicate the involvement of CREB in LTM. Thus, deficient LTM in our *CBP*$^{+/-}$ mice could be caused partly by deficient CREB-dependent transcription. In such a case, signal transduction functions downstream of CREB binding are considered to be defective, as the CREB-binding domain is included in the truncated CBP. CREB is almost certainly not the only transcription factor modulating the induction of protein synthesis required for LTM. It is highly likely that other transcription factors, which bind functional domains in the truncated protein or on its C-terminal side, also have some role in LTM. It is possible that the insufficient amount of CBP influences brain development, possibly the hippocampus (28), which is thought to be involved in memory storage. However, microscopic analyses of the forebrain of *CBP*$^{+/-}$ mice did not reveal any anatomical abnormalities (data not shown).

In RTS patients, the ratio of cardiac abnormalities is ~33%, with patent ductus arteriosus and VSD as the most common defects (1,29). In the present study, the survival ratio of *CBP*$^{+/-}$ mice was significantly low when compared with *CBP*$^{+/+}$ littermates at 3 weeks after birth. Fetuses at 19.5 d.p.c. were investigated for heart anomalies. Approximately 17% of *CBP*$^{+/-}$ fetuses had congenital heart defects, mainly membranous-type VSD. This finding suggests that cardiac anomaly is one of the reasons for death after birth. Our homozygous CBP mutant fetuses (Y. Oike *et al*., submitted for publication) are embryonic lethal with abnormalities of vascular network formation, especially abnormal development of endothelial cells which could cause the membranous-type VSD observed.

Our *CBP*$^{+/-}$ mice showed more severe phenotypes as well as greater penetrance compared with the *CBP*$^{+/-}$ null mice of Tanaka *et al.* (12). *CBP*$^{+/-}$ null mice exhibited growth retardation (7/21 mice, 33%) and skeletal abnormalities, such as large anterior fontanel (67%) and distinct holes in the xiphoid process (29%), while our *CBP*$^{+/-}$ mice showed growth retardation (100%), retarded osseous maturation (100%), large anterior fontanel (100%), hypoplastic maxilla with narrow palate (100%), cardiac anomalies (17%), skeletal abnormalities (7%) and occasional seizures. In addition, poor locomotor activity (100%) and LTM deficits (100%), which Tanaka *et al.* have not studied, were also observed in our *CBP*$^{+/-}$ mice. Tanaka *et al.* used TT2 ES cells (14) to generate a male chimera, and it then was bred with BALB/c or C57BL/6 females to produce *CBP*$^{+/-}$ mice. They claim that phenotypes were milder in *CBP*$^{+/-}$ mice obtained by mating with C57BL/6 mice than those with BALB/c mice. In our experiment, the same TT2 ES cell line was used for mutant generation, and generated mutants were mated with C57BL/6 mice. The genetic background in Tanaka's and our mutants is not completely identical as the TT2 cell line used in both studies was derived from an F_1 cross of C57BL/6 and CBA mice. Thus true comparisons between the two types of CBP mutants will have to await the time when both mutations are on a pure genetic background after repeated backcrosses. However, it still stands that the main difference between Tanaka's and our mutants is the presence of truncated CBP in our *CBP*$^{+/-}$ mice. Our *CBP*$^{+/-}$ mice correlate much more closely with RTS phenotypes than do *CBP*$^{+/-}$ null mice.

The evidence that RTS is a consequence of reduced amounts of CBP is based on RTS cases resulting from heterozygous defects of *CBP* (5). This indicates that two copies are needed for normal development. Diseases due to this type of mechanism fall into at least three different categories of mutation: transcription factors, receptors and signal transduction molecules, and structural molecules (30). For transcription factors, it seems likely that some developmental pathways are particularly susceptible to dosage effects because of their exquisite sensitivity to levels of certain critical proteins. It is also conceivable that the smaller the amount of CBP, the more severe the phenotype that could result. Theoretically, gene dosage should be 50% of normal in a haplo-insufficiency mechanism. On the other hand, in a dominant-negative mechanism, it should be 0–50% of normal. Our homozygous *CBP* mutant fetuses, which have no CBP (0%) and thus the most severe form, died between 9.5 and 10.5 d.p.c.

A dominant-negative effect of CREB-binding peptide (amino acids 455–679) on cAMP-responsive transcription and nuclear receptor-activated transcription was well established by nuclear microinjection experiments (11,13). These results indicate competitive binding between wild-type CBP and CREB-binding peptide.

In order to show clearly that the allele for this truncated CBP is an antimorph (dominant-negative) and not a neomorph (a new gene product) (31), we need to demonstrate that the heterozygous mice with our CBP truncated allele and a null allele have a more severe phenotype than our *CBP*$^{+/-}$ truncated mutant. Homozygous *CBP* mutant fetuses, both those used by us and those of Tanaka, died between 9.5 and 10.5 d.p.c. This indicates very strongly that a heterozygous CBP truncated allele/null allele mouse would be embryonic lethal.

Taken together, the observed phenotypic differences between the *CBP*$^{+/-}$ null (12) and our *CBP*$^{+/-}$ truncated mutant could be explained by the dominant-negative action of truncated protein. In other words, Tanaka's mice can be explained by a haplo-insufficiency mechanism, and ours by a dominant-negative mechanism. The most likely explanation is that the truncated CBP competitively binds CREB and inactivates it. However, other effects of the truncated CBP cannot be ruled out.

The wide variation in the severity of mental retardation and in the expression of physical features observed in RTS patients could be partly explained by the differences seen in the haplo-insufficiency and dominant-negative mechanisms in mice. Human studies of RTS patients using the *RT1* probe, which contains the 3′ end of *CBP*, have been done (5,32–34). From the four studies, ~12% of the RTS patients studied are found to have submicroscopic genomic deletions. In one study (5), some of the patients in this 12% were analyzed in more detail, and a wide variety of partial *CBP* deletion mutants were observed. It is highly likely that some of these patients express truncated CBP. Although it is claimed that there is no obvious phenotypic difference between patients with or without the *RT1* deletion, it is still possible that variations in haplo-insufficiency and dominant-negative mutants lead to the various observed RTS severities. Further molecular analysis of RTS cases is needed for clarification of the genetic etiology of the syndrome.

A well understood example of transcription factor variation in haplo-insufficiency and dominant-negative mutants leading to a broad range of disease severity is seen for the *WT1* (35) and *GLI3* (36) genes. For the *WT1* gene, WAGR syndrome (Wilms' tumor, aniridia, genitourinary anomalies and mental retardation) is caused by a haplo-insufficiency mechanism, and Denys–Drash syndrome (typical nephropathy, genital abnormalities and Wilms' tumor) by a dominant-negative mechanism. In the same manner, mutations in the *GLI3* gene are responsible for two syndromes: Greig cephalopolysyndactyly syndrome by a haplo-

insufficiency mechanism and Pallister–Hall syndrome by a dominant-negative mechanism. Patients with either syndrome show polysyndactyly and abnormal craniofacial features, with Pallister–Hall syndrome showing a greater severity. These examples of other transcription factors highlight the possibility that RTS is also under a similar control.

The role of CBP in embryogenesis and morphogenesis is currently unknown. CBP is known to be involved in RTS. RTS has multiple phenotypes which suggest that CBP plays a variable and vital role in various basic developmental functions, as would be expected of such a promiscuous transcription factor. Our *CBP*$^{+/-}$ mice exhibit all of the phenotypes associated with human RTS except broad thumbs and broad halluces. Thus, our *CBP*$^{+/-}$ mice would be an excellent model for the study of the role of CBP in development and mental retardation.

MATERIALS AND METHODS

Construction of a trapping vector

The pU-San trapping vector was generated by inserting two *lox*P sequences, one at each of the *Pst*I and *Sma*I sites of pUC19, and a *Sal*I fragment containing the splice acceptor (SA) region from the mouse *Engrailed-2* (*En-2*) gene ligated with a reporter gene was inserted at the *Sal*I site of the above construct. A *Sal*I reporter gene fragment derived from another trapping vector, pGT1.8IresβgeO (kindly provided by Dr Austin Smith, University of Edinburgh, UK), which has an internal ribosomal entry site (IRES), a β-galactosidase/neomycin phosphotransferase fused gene (β-geo) and an SV40 polyadenylation sequence, was also ligated into one of the *Sal*I sites to generate pU-San (Fig. 1a). pU-San linearized with *Spe*I was introduced into ES cells by electroporation.

Generation of mutant mice by gene trapping

An ES cell line, TT2 (14) (kindly provided by Dr Shinichi Aizawa, Kumamoto University, Japan), derived from an F_1 embryo crossed between a C57BL/6 female and a CBA male, was used for gene trapping. The cells were maintained as described (37). Thirty micrograms of the *Spe*I-linearized pU-San were electroporated into 10^7 ES cells at 960 μF, 500 V/cm. The trapped ES cells were selected with G418 at 150 μg/ml for 10 days and isolated for further analyses. Chimeras were produced by injection of isolated trapped ES cells, which had only a single copy of the vector integrated, into eight-cell embryos (37). The mice were housed in environmentally controlled rooms of the Laboratory Animal Research Center of Kumamoto University Medical School under the guidelines of Kumamoto University for animal and recombinant DNA experiments. Embryos, newborn and adult mice were genotyped by Southern blot analyses of tail DNA. For Southern analyses, genomic DNA was digested with *Eco*RI and resolved on 0.8% agarose gels.

Characterization of the disrupted genomic region

The 5′-RACE PCR method using the 5′ RACE system (BRL, Gaithersburg, MD), the 5′ side plasmid rescue method (38) using the CRE–*lox*P system (39) and the 3′ side plasmid rescue method were employed to characterize the genomic region where the trapping vector was inserted. For the 5′-RACE method, two oligonucleotide primers of the *En-2* genomic region were used as follows: 5′-TGCTCTGTCAGGTACCTGTTGG-3′ for reverse transcription and 5′-CTTTGTTAGGGTTCTTCTTC-3′ for PCR. To isolate wild-type genomic clones, a mouse BAC PCRable DNA pool (Genome Systems, St Louis, MO) was screened by PCR using primers of rescued genomic flanking region. A 7.5 kb *Eco*RI fragment of isolated BAC CBP clones was subcloned into pBluescript II SK (Stratagene, La Jolla, CA) and the resulting plasmid was used to characterize the genomic region by restriction mapping and sequencing the exon–intron structure located on the 5′ side of the inserted region.

Western blotting

Brain homogenates from *CBP*$^{+/+}$ and *CBP*$^{+/-}$ adult mice were prepared as previously described (40). SDS–PAGE of 30 μg of brain homogenate protein using 7.5% gels was performed. Proteins were then transferred to a nitrocellulose filter (Millipore, Bedford, MA), and detected using anti-CBP (CBP-A22 or CBP-C20; Santa Cruz Biotechnology, Santa Cruz, CA) antibodies (5) and the ECL detection system (Amersham, Arlington Heights, IL).

Morphological analyses of skeletons and heart

The skeletons of adult mice were analyzed radiographically using the μFX-1000 system (Fujifilm, Tokyo, Japan), and these images were analyzed using the BAS 5000 system (Fujifilm).

Pregnant mice were sacrificed at 19.5 d.p.c. and the numbers of fetuses were recorded. Each fetus was fixed in Bouin's fixative and hearts were dissected according to the technique of Barrow and Tatlor (41).

Locomotor activity

Locomotor activity was determined for a 60 min period, employing an animal movement analyzing system with photocell counter (Scanet SV-10; Toyo Sangyo, Toyama, Japan) as previously reported (17). The apparatus was placed in a closed box, to exclude light, noise, smells, etc. The movements of each mouse were counted automatically every 5 min for 60 min.

Spontaneous alternation behavior in a Y-maze

The apparatus and the procedure were basically the same as previously reported (18). In brief, each mouse was placed at the end of one arm and allowed to explore the maze freely for 8 min. Alternation was defined as successive entries into the three arms, on overlapping triplet sets. The percentage alternation was calculated as the ratio of actual to possible alternations (defined as the total number of arm entries minus two) multiplied by 100. Arm entry was considered to be completed when the hind paws of the mouse had been completely placed in the arm.

Water maze test

The apparatus used was previously described (19). Our pool was 1.2 m in diameter and was made of white polypropylene plastic, and water in the pool was kept at 18.5 ± 0.5°C. The test subjects were kept on shelves underneath the pool to eliminate directional olfactory and auditory cues. The plexiglas platform was 7 cm in diameter, and its surface was 2 cm below the surface of the water to help the mice to climb onto it. The room had adjustable indirect illumination. A camera was fixed to the ceiling of the room.

Swimming paths were tracked with the camera and stored in a computer (TARGET/2 system; Neuroscience, Tokyo, Japan). The mice did not swim in the pool before training (i.e. there was no habituation). During training in the hidden platform test of the water maze, the platform was not marked by any cue, and it was kept in the same place throughout training. In a block of trials, the starting position of the mice was varied pseudorandomly so as to ensure that three starting positions were used. If the mouse found the platform, it was allowed to remain there for 30 s and was then returned to its home cage. If the mouse was unable to find the platform within 60 s, the training session was terminated and a maximum score of 60 s was assigned. Training was conducted on 10 consecutive days, three times a day. A transfer test was given on the 13th day, and mice swam for 60 s in the absence of the platform.

Step-through-type passive avoidance test

The apparatus used was described previously (18,19). This test consisted of two trials. In the acquisition trial, mice were placed individually in lighted compartments. Ten seconds later, the door to the dark compartment was opened, and the latency until the mouse entered the dark compartment was recorded. When the animal had stepped through the door, the door was closed, and an electric shock (0.2 mA, 2 s) was delivered via the grid floor. The mouse was removed after receiving the footshock and placed back into the light compartment by the experimenter. The door was again opened 10 s later to start the next trial. Training continued in this manner until the mouse stayed in the light compartment for 120 s in a single trial. Twenty four hours later, each animal was placed in the light compartment and the step-through latency was recorded until 300 s had elapsed (retention trial).

Fear conditioning

Our conditioning chamber was in a soundproof box ($90 \times 65 \times 60$ cm). Surrounding noise measured 75 dB, while that within the box registered 68 dB. To provide background white noise (72 dB), a single computer fan was installed in one of the sides of the isolation chamber. The conditioning chamber ($25 \times 30 \times 47$ cm) is made of transparent Plexiglas. The chamber has a 27-bar insulated shock grid floor. The floor is removable and, after each experimental subject, it was cleaned with 70% ethanol. Each bar (1.5 mm in diameter) is connected through a harness to a Shockgenerator (NS-SG01; Neuroscience), a device that delivers scrambled shocks. The speaker used to deliver the conditioned stimulus (CS) is connected to a power supply with an adjustable current output that was kept constant throughout the experiments. Only one subject at a time was present in the experimentation room. The other subjects remained in their home cages. Each subject was carried to the behavioral room in a cage with shavings from its home cage, and the proceedings were filmed. For the cued and contextual conditioning experiments, mice were placed in the conditioning chamber for 2 min before the onset of the discrete CS (30 s at 2800 Hz and 85 dB of sound). In the last 2 s of CS, they were exposed to the unconditioned stimulus (US) (at 0.8 mA for 2 s of continuous foot shock). After the CS–US pairing, the mice were left in the conditioning chamber for another 30 s and were then placed back in their home cages. For contextual conditioning, freezing was measured for 5 min (consecutive) in the chamber in which the mice had trained. In this study, we analyzed the freezing behavior measured automatically by Scanet SV10-AQ (Toyo Sangyo). Groups 1, 2 and 3 were tested at 0.5, 1 and 24 h after training, respectively. In cued conditioning, the mice were placed in a novel context (new plastic cage with soft floor) for 3 min (pre-CS test), after which they were exposed to the CS for 3 min (CS test). Groups 1, 2, 3 and 4 were tested 0.5, 1, 6 and 24 h after training, respectively.

Statistical analyses

All results are expressed as means ± SEM for each group. In the step-through-type passive avoidance test, statistical analysis of differences between groups was performed with Dunnett's multiple comparisons test. For the analysis of fear conditioning experiments, we used analysis of variance (ANOVA) with repeated measures and ANOVA with dependent measures. In analysis for growth, an unpaired Student's *t*-test was used to compare values between $CBP^{+/+}$ and $CBP^{+/-}$ littermates. In analyses of heart anomalies, Fisher's exact probability test was used to compare values between $CBP^{+/+}$ and $CBP^{+/-}$ littermates. Differences were considered statistically significant at a level of $P < 0.05$.

ACKNOWLEDGEMENTS

We thank Dr John F. Maune for critical assistance in manuscript preparation, Dr T. Miyakawa and S. Oku for helpful advice, and Dr N. Hiro-oka, Dr M. Akizuki, Ms Y. Kiyonaga and Ms M. Tokushima for experimental assistance. This work was supported by Grants-in-Aid for Scientific Research on Priority Areas from the Ministry of Education, Science and Culture of Japan.

ABBREVIATIONS

CBP, CREB-binding protein; CREB, cyclic AMP response element-binding protein; LTM, long-term memory; RTS, Rubinstein–Taybi syndrome; STM, short-term memory; VSD, ventricular septal defect.

REFERENCES

1. Jones, K.L. (1988) *Smith's Recognizable Patterns of Human Malformation*, 4th edn. W. B. Saunders, Philadelphia, PA, pp. 84–87.
2. Hennekam, R.C.M., Stevens, C.A. and Van de Kamp, J.J.P. (1990) Etiology and recurrence risk in Rubinstein–Taybi syndrome. *Am. J. Med. Genet.*, **6** (suppl.), 54–64.
3. Padfield, C.J., Partington, M.W. and Simpson, N.E. (1968) The Rubinstein–Taybi syndrome. *Arch. Dis. Child.*, **43**, 94–101.
4. Chrivia, J.C., Kwok, R.P.S., Lamb, N., Hagiwara, M., Montominy, M.R. and Goodman, R.H. (1993) Phosphorylated CREB binds specifically to the nuclear protein CBP. *Nature*, **365**, 855–859.
5. Petrij, F., Giles, R.H., Dauwerse, H.G., Saris, J.J., Hennekam, R.C.M., Masuno, M., Tommerup, N., van Ommen, G.B., Goodman, R.H., Peters, D.J.M. and Breuning, M.H. (1995) Rubinstein–Taybi syndrome caused by mutations in the transcriptional co-activator CBP. *Nature*, **376**, 348–351.
6. Kwok, R.P.S., Lundblad, J.R., Chrivia, J.C., Richards, J.P., Bachinger, H.P., Brennan, R.G., Roberts, S.G.E., Green, M.R. and Goodman, R.H. (1994) Nuclear protein CBP is a coactivator for the transcription factor CREB. *Nature*, **370**, 223–226.
7. Bannister, A.J. and Kouzarides, T. (1995) CBP-induced stimulation of c-Fos activity is abrogated by E1a. *EMBO J.*, **14**, 4758–4762.
8. Arias, J., Alberts, A.S., Brindle, P., Claret, F.X., Smeal, T., Karin, M., Feramisco, J. and Montominy, M. (1994) Activation of cAMP and mitogen responsive genes relies on a common nuclear factor. *Nature*, **370**, 226–229.

9. Dai, P., Akimura, H., Tanaka, Y., Hou, D., Yasukawa, T., Kanei-Ishii, C., Takahashi, T. and Ishii, S. (1996) CBP as a transcriptional coactivator of c-Myb. *Genes Dev.*, **10**, 528–540.
10. Kamei, Y., Xu, L., Heinzel, T., Torchia, J., Kurokawa, R., Gloss, B., Lin, S., Heyman, R.A., Rose, D.W., Glass, C.K. and Rosenfeld, M.G. (1996) A CBP integrator complex mediates transcriptional activation and AP-1 inhibition by nuclear receptors. *Cell*, **85**, 403–414.
11. Chakravarti, D., Lamorte, V.J., Nelson, M.C., Nakajima, T., Schulman, I.G., Juguilon, H., Montominy, M. and Evans, R.M. (1996) Role of CBP/P300 in nuclear receptor signalling. *Nature*, **383**, 99–103.
12. Tanaka, Y., Naruse, I., Maekawa, T., Masuya, H., Shiroishi, T. and Ishii, S. (1997) Abnormal skeletal patterning in embryos lacking a single *Cbp* allele: a partial similarity with Rubinstein–Taybi syndrome. *Proc. Natl Acad. Sci. USA*, **94**, 10215–10220.
13. Parker, D., Ferreri, K., Nakajima, T., LaMorte, V.J., Evans, R., Koerber, S.C., Hoeger, C. and Montominy, M.R. (1996) Phosphorylation of CREB at Ser-133 induces complex formation with CREB-binding protein via a direct mechanism. *Mol. Cell. Biol.*, **16**, 694–703.
14. Yagi, T., Tokunaga, T., Furuta, Y., Nada, S., Yoshida, M., Tsukada, T., Saga, Y., Takeda, N., Ikawa, Y. and Aizawa, S. (1993) A novel ES cell line, TT2, with high germline-differentiating potency. *Anal. Biochem.*, **214**, 70–76.
15. Gossler, A., Joyner, A.L., Rossant, J. and Skarnes, W.C. (1989) Mouse embryonic stem cells and reporter constructs to detect developmentally regulated genes. *Science*, **244**, 463–465.
16. Skarnes, W.C., Auerbach, B.A. and Joyner, A.L. (1992) A gene trap approach in mouse embryonic stem cells: the *lacZ* reporter is activated by splicing, reflects endogenous gene expression, and is mutagenic in mice. *Genes Dev.*, **6**, 903–918.
17. Noda, Y., Yamada, K., Furukawa, H. and Nabeshima, T. (1995) Enhancement of immobility in a forced swimming test by subacute or repeated treatment with phencyclidine: a new model of schizophrenia. *Br. J. Pharmacol.*, **116**, 2531–2537.
18. Yamada, K., Noda,Y., Hasegawa, T., Komori, Y., Nikai, T., Sugihara, H. and Nabeshima, T. (1996) The role of nitric oxide in dizocilpine-induced impairment of spontaneous alternation behavior in mice. *J. Pharmacol. Exp. Ther.*, **276**, 460–466.
19. Manabe, T., Noda, Y., Mamiya, T., Katagiri, H., Houtani, T., Nishi, M., Noda, T., Takahashi, T., Sugimoto, T., Nabeshima, T. and Takeshima, H. (1998) Facilitation of LTP and memory in mice lacking nociceptin receptor. *Nature*, **394**, 577–581.
20. Sarter, M., Bodewitz,G. and Stephens, D. (1988) Attenuation of scopolamine-induced impairment of spontaneous alternation behavior by antagonist but not inverse agonist and agonist carbolines. *Psychopharmacology*, **94**, 491–495.
21. Parad-Turska, J. and Turski, W.A. (1990) Excitatory amino acid antagonists and memory: effects of drugs acting at *N*-methyl-D-aspartate receptors in learning and memory tasks. *Neuropharmacology*, **29**, 1111–1116.
22. Stone, W.S., Walser, B., Gold, S.D. and Gold, P.E. (1991) Scopolamine- and morphine-induced impairment of spontaneous alternation performance in mice: reversal with glucose and with cholinergic and adrenergic agonists. *Behav. Neurosci*., **105**, 264–271.
23. Bourtchuladze, R., Frenguelli, B., Blendy, J., Cioffi, D., Schutz, G. and Silva, A.J. (1994) Deficient long-term memory in mice with a targeted mutation of the cAMP-responsive element-binding protein. *Cell*, **79**, 59–68.
24. Bartsch, D., Ghirardi, M., Skehel, P.A., Karl, K.A., Herder, S.P.,Chen, M., Bailey C.H. and Kandel, E.R. (1995) *Aplysia* CREB2 represses long-term facilitation: relief of repression converts transient facilitation into long-term functional and structural change. *Cell*, **83**, 979–992.
25. Tully, T., Preat, T., Boynton, S.C. and Del Vecchio, M. (1994) Genetic dissection of consolidated memory in *Drosophila*. *Cell*, **79**, 35–47.
26. Yin, J.C.P., Wallach, J.S., Vecchio, M.D., Wilder, E.L., Zhou, H., Quinn, W.G. and Tully, T. (1994) Induction of a dominant negative CREB transgene specifically blocks long-term memory in *Drosophila*. *Cell*, **79**, 49–58.
27. Yin, J.C.P., Del Vecchio, M., Zhou, H. and Tully, T. (1995) CREB as a memory modulator: induced expression of a *dCREB2* activator isoform enhances long-term memory in *Drosophila*. *Cell*, **81**, 107–115.
28. Eichenbaum, H., Otto, T. and Cohen, N.J. (1992) The hippocampus—what does it do? *Behav. Neural Biol*., **57**, 2–36.
29. Stevens, C.A. and Bhakta, M.G. (1995) Cardiac abnormalities in the Rubinstein–Taybi syndrome. *Am. J. Med. Genet.*, **59**, 346–348.
30. Fisher, E. and Scambler, P. (1994) Human haploinsufficiency—one for sorrow, two for joy. *Nature Genet*., **7**, 5–7.
31. Muller, H.J. (1932) Further studies on the nature and causes of gene mutations. *Sixth International Congress of Genetics*, Brooklyn Botanic Gardens, Ithaca, NY, pp. 213–255.
32. Hennekem, R.C., Tilanus, M., Hamel, B.C., Voshart-van, H.H., Mariman, E.C., van Beersum, S.E., van den Boogaard, M.J. and Breuning, M.H. (1993) Deletion at chromosome 16p13.3 as a cause of Rubinstein–Taybi syndrome: clinical aspects. *Am. J. Hum. Genet.*, **52**, 255–262.
33. Wallerstein, R., Anderson, C.E., Hay, B., Gupta, P., Gibas, L., Ansari, K., Cowchock, F.S., Weinblatt, V., Reid, C., Levitas, A. and Jackson, L. (1997) Submicroscopic deletions at 16p13.3 in Rubinstein–Taybi syndrome: frequency and clinical manifestations in a North American population. *J. Med. Genet.*, **34**, 203–206.
34. Taine L., Goizet, C., Wen, Z.Q., Petrij, F., Breuning, M.H., Ayme, S., Saura, R., Arveiler, B. and Lacombe, D. (1998) Submicroscopic deletion of chromosome 16p13.3 in patients with Rubinstein–Taybi syndrome. *Am. J. Med. Genet.*, **78**, 267–270.
35. Hastie, N.D. (1992) Dominant negative mutations in the Wilms tumour (*WT1*) gene cause Denys–Drash syndrome—proof that a tumour-suppressor gene plays a crucial role in normal genitourinary development. *Hum. Mol. Genet.*, **1**, 293–295.
36. Kang, S., Graham, J.M. Jr, Olney, A.H. and Biesecker, L.G. (1997) *GLI3* frameshift mutations cause autosomal dominant Pallister–Hall syndrome. *Nature Genet.*, **15**, 266–268.
37. Yagi, T., Noda, S., Watanabe, N., Tamemoto, H., Kohmura, N., Ikawa, Y. and Aizawa, S. (1993) A novel negative selection for homologous recombinants using diphtheria toxin A fragment gene. *Anal. Biochem.*, **214**, 77–86.
38. Niwa, H., Araki, K., Kimura, S., Taniguchi, S., Wakasugi, S. and Yamamura, K. (1993) An efficient gene-trap method using poly A trap vectors and characterization of gene-trap events. *J. Biochem.*, **113**, 343–349.
39. Araki, K., Imaizumi, T., Okuyama, K., Oike, Y. and Yamamura, K. (1997) Efficiency of recombination by cre transient expression in embryonic stem cells: comparison of various promoters. *J. Biochem*., **122**, 977–982.
40. Gorski, K., Carneiro, M. and Schibler, U. (1986) Tissue-specific *in vitro* transcription from the mouse albumin promoter. *Cell*, **47**, 767–776.
41. Barrow, M.V. and Taylor, W.J. (1969) A rapid method for detecting malformations in rat fetuses. *J. Morphol*., **127**, 291–306.